MAGMA (2004) 17: 219–228
DOI 10.1007/s10334-004-0071-7

RESEARCH ARTICLE

Evaluation of cartilage repair tissue after biomaterial implantation in rat patella by using T2 mapping

A. Watrin-Pinzano
J.-P. Ruaud
Y. Cheli
P. Gonord
L. Grossin
I. Bettembourg-Brault
P. Gillet
E. Payan
G. Guillot
P. Netter
D. Loeuille

Received:12 May 2004
Revised:27 September 2004
Accepted: 27 September 2004
Published online: 1 December 2004

A. Watrin-Pinzano · Y. Cheli · L. Grossin
P. Gillet (✉) · E. Payan · P. Netter
Department of Pharmacology,
UMR 7561 CNRS - Nancy I
"Physiopathologie et Pharmacologie Articulaires" Faculté de Médecine,
BP 184, Avenue de la Forêt de Haye
F54505 Vandoeuvre-les-nancy, France
Tel.: +33-(0)-383683950
Fax : +33-(0)-383683959
E-mail :
Pierre.Gillet@medecine.uhp-nancy.fr

J. P. Ruaud · P. Gonord · G. Guillot
UMR 8081 CNRS – Université Paris-Sud,
"Unité de Recherche en Résonance Magnétique Médicale (U2R2M),
Orsay Cedex, 91405 France

I. Bettembourg-Brault · D. Loeuille
Departments of Rheumatology and Pharmacology
Hôpitaux de Brabois,
Vandoeuvre-les-Nancy,
54505 France

Abstract To evaluate the ability of MR T2 mapping (8.5 T) to characterize ex vivo longitudinally, morphologically and quantitatively, alginate-based tissue engineering in a rat model of patellar cartilage chondral focal defect. Calibrated rat patellar cartilage defects (1.3 mm) were created at day 0 (D0) and alginate sponge with (Sp/C+) or without (Sp/C−) autologous chondrocytes were implanted. Animals were sacrificed sequentially at D20, D40 and D60 after surgery and dissected patellae underwent MRI exploration (8.5 T). T2 values were calculated from eight SE images by using nonlinear least-squares curve fitting on a pixel-by-pixel basis (constant repetition time of 1.5 s, eight different echo times: 5.5, 7.5, 10.5, 12.5, 15.0, 20.0, 25.0 and 30.0 ms). On the T2 map, acquired in a transversal plane through the repair zone, global T2 values and zonal variation of T2 values of repair tissue were evaluated versus control group and compared with macroscopic score and histological studies (toluidine blue, sirius red and hematoxylin-eosin). "Partial", "total" and "hypertrophic" repair patterns were identified. At D40 and D60, Sp/C+ group was characterized by a higher proportion of "total" repair in comparison to Sp/C− group. At D60, the proportion of "hypertrophic" repair was two fold in Sp/C− group versus Sp/C+ group. As confirmed morphologically and histologically, the T2 map also permitted the distinction of three types of repair tissue: "total", "partial" and "hypertrophic". "Total" repair tissue was characterized by high T2 values versus normal cartilage ($p < 0.05$). Zonal variation, reflecting the collagen network organization, appeared only at D60 for Sp/C+ group ($p < 0.05$). "Hypertrophic" tissue, mainly observed at D60, presented high T2 global values without zonal variation with cartilage depth. These results confirm the potency of the MR T2 map (8.5 T) to characterize macroscopically and microscopically the patterns of the scaffold guided-tissue repair of a focal chondral lesion in the rat patella ("total", "partial" and "hypertrophic"). On T2 map, three parameters (i.e. MRI macroscopic pattern, T2 global values and zonal variation of T2 values) permit to characterize chondral repair tissue, as a virtual biopsy.

Keywords Magnetic resonance imaging · T2 mapping · Chondrocyte · Cartilage repair · Chondral lesion

Introduction

Articular cartilage is an avascular, non-innerved tissue and the resident cells, the chondrocytes, surrounded by a rich extracellular matrix, are unable to migrate to a chondral lesion site from an adjacent intact healthy site. This characteristic concerning hyaline articular cartilage leads to a poor intrinsic ability to heal itself. Degenerative chondral lesions are secondary to a large breakdown of cartilage, mainly observed in older patients (osteoarthritic disease) or to focal cartilage defects, after traumatic injuries in younger patients. The spontaneous repair of articular cartilage is only associated with transfixing defects penetrating subchondral bone and bone marrow space. In this case, a blood clot is formed, consisting of a fibrin matrix with various proteins, and different growth factors and blood cells secondly generate a spontaneous repair tissue. This new tissue, so called cicatricial fibrocartilage, contains predominantly type I collagen and exerts different biomechanical properties versus native tissue, thus undergoing progressive degeneration especially in weight-bearing areas.

Cartilage repair is a challenging clinical problem. Various surgical techniques have been proposed for the treatment of articular cartilage defects [1], but with limited success and a lack of long-term evaluation. Additionally, most of these studies report a progressive worsening of the cartilage lesions. Actually, in clinical practice, the gold-standard method to depict and to evaluate cartilage lesions according to their severity, surface and topography remains arthroscopy [2]. But this invasive procedure limits a longitudinal study over a short time period. In contrast, MRI is a non-traumatic technique permitting a direct visualization of different structures of the joint, and more particularly the cartilage tissue. Thus, MRI offers an opportunity to follow the progression of cartilage lesions [3, 4], to depict subchondral and trabecular bone modifications as well as synovial inflammation, and also to evaluate surgical procedures.

Experimental models of focal lesions of patellar cartilage have been previously developed by our group to perform tissue characterization of the reparation process by using concomitant MRI, macroscopic and microscopic studies [5]. Additionally, this multimodal longitudinal assessment in rat knee permits the evaluation of the accuracy of new biomaterials and to follow the main steps of the graft rebuilding, both being not ethically feasible in the clinics.

Following a recent detailed ex vivo study of transverse relaxation in human articular cartilage [6] the dominant mechanisms of $T_{1\rho}$ and T_2 are considered to be dipolar interaction due to slow anisotropic motion of water molecules in the collagen matrix. These mechanisms are sensitive to orientation of the collagen fibers relative to the magnetic field, with faster relaxation for fibers parallel to the magnetic field (0° orientation), slower at 90°, and the slowest at the magic angle (55°), the orientation effect being more visible in the radial zone with regular fiber orientation, than in the transitional zone of variable fiber orientation. One expects that this mechanism will be independent of magnetic field intensity. MR experiments in higher magnetic fields are intrinsically of interest to improve signal-to-noise ratio, and thus attainable spatial resolution.

The aim of this pilot study was to evaluate the chondrogenic potential of the graft of a purpose-made sponge (alginate and hyaluronate), colonized or not with autologous chondrocytes, in resurfacing full thickness defects of rat patellar cartilage. The different steps of the graft rebuilding were explored at various times (D20, D40 and D60) with a new quantitative technique (T2 map) which permits the evaluation of the structural organization and the matrix content of the rat patellar cartilage. On T2 map, the matrix content of the graft was evaluated by T2 global value assessments and the collagen network organization by zonal T2 value variations. After the MRI exploration, each patella was scored macroscopically and microscopically.

Materials and methods

Animals

Sixty five adult male Wistar rats (10-week-old animals) underwent surgically a focal calibrated defect of their right patellar articular cartilage according to a validated procedure [5]: 18 rats were implanted with alginate sponges enriched with hyaluronate alone (Sp/C−), and 23 rats were implanted with alginate sponges enriched with hyaluronate and autologous chondrocytes (Sp/C+). Patellae were longitudinally studied at three different time points of repair: D20 (Sp/C− n=5; Sp/C+ $n=7$), D40 (Sp/C− $n=6$; Sp/C+ $n=8$), and D60 (Sp/C− $n=7$; Sp/C+ $n=8$). Control rats ($n=24$) were sacrificed on D20, D40 and D60 to avoid bias inherent to the maturation process.

Sponge preparation

Sponges were prepared with a mixture containing sodium alginate from *Laminaria hyperborean* (20 g/l, Pronova), and hyaluronic acid from cocks comb (6.6 g/l, Sigma) in bi-distilled water. A 100-mM $CaCl_2$ solution was dripped under gentle magnetic stirring in these polysaccharide solutions (20 ml). After 30 min, the excess of calcium chloride solution was discarded and the sponge-shaped biomaterial was washed twice with 0.9% NaCl, frozen at −20°C and freeze-dried at −60°C under vacuum (Fisher Heto FD3 freeze-dryer, France) during 48 h. Finally, sponges were punched with a 6-mm biopsy pen (Stiefel, Germany) and autoclaved at 121°C for 20 min. For the sponge group, the sponge was hydrated with physiological serum before implantation inside the patellar cartilage defect.

Sponge with autologous chondrocytes preparation

Sponges with autologous chondrocytes were prepared from isolated chondrocytes obtained from sternal cartilage. In the first step, rats were anesthetized and the sternal cartilage sample was taken in sterile conditions, and stored individually in physiological serum (B. Braun, Germany) containing penicillin (0.6%) and streptomycin (0.6%). The chondrocytes were liberated by sequential digestions with 0.15% pronase from *Streptomyces griseus* (Sigma-Aldrich, France) in 0.9% NaCl for 2 h at 37°C, and then after washing, with 0.2% collagenase B from *Clostridium histoliticum* (Boehringer-Mannheim, Germany) in Dulbecco's Modified Eagle's Medium (DMEM)/Nut mix F-12 medium (Gibco BRL) supplemented with penicillin, streptomycin, amphotericin B (0.6%) and glutamine during 12 h at 37°C. The cells were counted, centrifuged at 1200 rpm for 10 min and put in suspension in DMEM/F-12 medium in order to obtain a concentration of 60,000 cells/20 μl. The 6-mm sponge biopsies were placed in 24 well plates (Corning) on the basis of one sponge biopsy per well and each sponge was moistened with 20 μl of complete medium containing 60,000 cells/ml. The 24 well plates were incubated for 1 h (37°C and 5% CO_2) to promote chondrocyte adhesion within the sponge. Then, 2 ml of complete medium supplemented with 3-mM $CaCl_2$ were added in each well in order to preserve sponge structure and changed every three days during fifteen days.

Surgical procedure

Rats were anesthetized with an intraperitoneal injection of a mixture of acepromazine (1 mg/kg) and ketamine (38 mg/kg). Under rigorous aseptic conditions, a medial parapatellar incision was made and the patella was reverted through 180° to expose its articular surface. A 1.3-mm-wide defect was drilled in the middle part of the patella from its surface until the subchondral bone. Before implantation, all sponges (with or without chondrocytes) were punched with a 2-mm biopsy pen (Stiefel, Germany). Following the groups, the defect was filled with sponges with or without chondrocytes. The patella was then repositioned and the periarticular muscles were repaired with Ethicon Vicryl (Johnson and Johnson Intl., Belgium) sutures and the skin closed with Polyamide Filapeau (Peters, France) sutures. The limb was not immobilized and the animals were allowed free-cage activity. The maintenance and care were respected as mentioned in the National Institutes of Health guidelines. At each time (D20, D40 and D60), animals were anesthetized and killed by cervical dislocation, knees were carefully dissected and kept frozen until MR study since preliminary studies showed that this procedure did not alter MR signal.

MR imaging and T2 mapping of rat patellar cartilage

The thawed patellae were dissected from the knee just before MR imaging exploration and placed for 16 h at 4°C in saline solution to correct the frozen process-related dehydration. Patellae were put into a closed atmosphere in a sample tube. All images were obtained with an 8.5-T MR micro-imager (Oxford instrument, Osney Head, England) with identical experimental parameters. Previously, a sagittal acquisition was done in order to localize the repair tissue. Then, the sequence of T2 mapping was acquired in a transversal plane through the repair tissue zone. All the patellae were oriented in the same direction in the sample tube placed inside the coil, with the superficial collagen fibers of patellar cartilage oriented perpendicular to the magnetic field strength. Eight spin-echo images were obtained with the following parameters: constant repetition time of 1.5 s; eight different echo times (5.5, 7.5, 10.5, 12.5, 15, 20, 25 and 30 ms); four signals acquired; total acquisition time 105 min; total bandwidth 27 kHz. The section thickness was 1 mm, the field of view was 4×4 mm, the matrix size was 128×128, yielding a pixel size of $31\times31\mu m^2$ over a slice thickness of 1 mm. The signal-to-noise ratio in cartilage pixels at the shortest echo time was typically 20. During MR imaging acquisitions, the magnet bore temperature varied between 25 and 30°C.

T2 values were calculated from the eight spin-echo images by using nonlinear least-squares curve fitting on a pixel-by-pixel basis. The signal intensity, SI, for the *i*th *j*th pixel as a function of time (t), can be expressed as follows: $SI_{ij}(t) = SO_{ij} \exp(-t/T2_{ij})$, where SO_{ij} is the pixel intensity at t = 0, and $T2_{ij}$ is the T2 time constant of the pixel ij. For pixels with signal intensity at the shortest echo time below three times the noise level (like air or bone pixels), or for pixels for which the fit algorithm did not converge properly (typically pixels in the trabecular region), the T2 values was set to zero. The T2 map was displayed on a pixel-by-pixel basis (Transform; Spyglass, Savoy, III) for the cartilage itself but also for adjacent structures such as subchondral and trabecular bone. The T2 maps were treated as two-byte integers over a range of 0–33 ms, which was known to be appropriate from previous experience on rat cartilage T2 values at a magnetic field intensity of 8.5 T. The color scale representation of the T2 maps was accordingly chosen over the same range.

Morphological analysis of T2 map

The air-cartilage interface was easily defined owing to the zero-T2 value set for air pixels. Conversely, both calcified cartilage and subchondral bone had low T2 values, which did not permit a clear delineation between both tissues. With this in mind, on T2 maps, the value of 4 msec was considered to be the lower threshold value for the deepest part of the non-calcified tissue.

In patellar cartilage repairs, three types of repaired tissue (Fig. 1) may be observed: "partial", "total" and "hypertrophic" repairs. On T2 mapping, these repair tissues were also delimited by superior and inferior borders.

- In "*partial repairs*", the superior border corresponded to a virtual line joining the superficial limits of the adjacent cartilage. The superficial limit of the repaired tissue was thus placed under the superior border.
- In "*total repairs*", the superior border corresponded to the superficial limit of the repaired tissue, which was located at the same level as the adjacent superficial cartilage.
- The "*hypertrophic repairs*" were characterized by a voluminous tissue formation localized over the adjacent cartilage, covering in some cases its surface. The superior border corresponded to the superficial limit of the hypertrophic tissue.

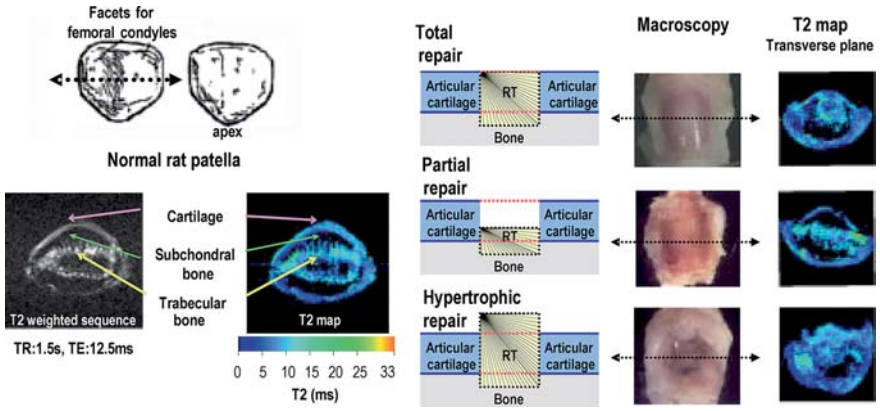

Fig. 1 MR patterns of normal rat patella (left, T2-weighted sequence and T2 map) and cartilage repair (D60, right). On each patella (internal macroscopical view) arrow represents the transversal plane for the MR T2 map scan. See the three types of macroscopic and MR patterns (8.5 T) of repair tissue: total, partial and hypertrophic repair tissues (RT)

In all repairs, the inferior border was not clearly identified and corresponded to a virtual line joining the adjacent subchondral bone.

Quantitative analysis of T2 map

The T2 global values of normal rat patellar cartilage and repair tissues were calculated as the mean of pixel values between these two borders (superior and inferior borders). Superficial and deep T2 values corresponded to the mean values of pixels that constituted the superior and inferior borders respectively. Thus, zonal variations in T2 values were appreciated as the difference between superficial and deep T2 values. Immediately after MRI exploration, patellae were fixed in formalin solution before macroscopic and microscopic analysis.

Macroscopical analysis

All patellae were observed on a binocular magnifying glass (×2) in order to score the repair tissues according to five parameters taking into account the quality of the filling tissue as previously described by Watrin-Pinzano et al. [5].

Histological analysis

Fixed patellae were decalcified for 1 h with Rapid Decalcifier RDO (Apex Engineering Products corporation, Canada), dehydrated and embedded in paraffin. Sections of 5 µm were cut in the transversal plane with a microtome, deparaffinized in toluene, and hydrated in a graded series of ethanol. The sections performed on repair tissue and normal cartilage (control group) were stained with hematoxylin-eosin (HES) to evaluate cellularity and morphologic aspect, with toluidine blue (TB) to evaluate proteoglycan content, and picrosirius red (SR) to evaluate collagen content. To examine the network organization in both groups, the SR sections were analyzed in polarized light microscopy. For each time point, the quality of the repair tissue was determined as previously described [5] according to 11 histological parameters aimed at appreciating morphological and structural organizations, cellular aspect, and distribution of matrix constituents in the repair tissue.

Statistical analysis

The differences between global, superficial and deep T2 values were analyzed by an ANOVA followed by a Fisher's t test and compared with a control group with a level of significance $\alpha \leq 0.05$. Concerning chondral repairs (three types of repairs per groups: "*total repair*", "*partial repair*" and "*hypertrophic repair*"), only groups made up by at least four patellae with an identical macroscopic pattern were considered for statistical evaluation.

Results

Macroscopy

At D20, repairs have been classified in two categories (Table 1): *"total repairs"* (Sp/C−: 40%; Sp/C+: 28.6%) and *"partial repairs"* (Sp/C− 60%; Sp/C+: 71.4%). For Sp/C− group, the *"total repairs"* zone appeared as a translucent tissue associated with an irregular aspect of its surface, clearly individualized from adjacent normal cartilage. In comparison, the Sp/C+ group is characterized by a hyaline cartilage pattern of the repaired zone with a rough and disorganized surface. *"Partial repairs"* presented, whatever the groups studied, a central hollow due to a lack of tissue repair.

At D40, the percentage of *"total repairs"* increased in the Sp/C+ group *versus* the Sp/C− group (87.5% vs 50%) (Table 1): the macroscopic score improved only for the Sp/C− group versus D20 (Sp/C−10 ± 1.0; Sp/C+ 8 ± 1.1). Furthermore, we noted an *"hypertrophic repair"* (12.5%) at this early time for the Sp/C+ group, while for the Sp/C− group we still noted *"partial repair"* (50%).

Table 1 Macroscopic sand histological scores of rat patellar repair tissue at D20, D40 and D60 according its classification (total, partial or hypertrophic repair tissue) and the implanted scaffold (Sp/C− = Sponge alone or Sp/C+ = Sponge seeded with autologous chondrocytes)

Types of repair		Total repair			Partial repair			Hypertrophic repair		
Time point	Groups	% of total repair	Macro score (/12)	Histo. score (/28)	% of partial repair	Macro score (/12)	Histo. score (/28)	% of hypertrophic repair	Macro score (/12)	Histo. score (/28)
D20	Sp/C−	40% ($n=2$)	5	12.5 ± 0.5	60% ($n=3$)	5.7 ± 0.9	10.3 ± 3.8	–	–	–
	Sp/C+	28.6% ($n=2$)	8.5 ± 0.5	13.0 ± 1.0	71.4% ($n=5$)	7.8 ± 0.7	12.4 ± 1.2	–	–	–
D40	Sp/C−	50% ($n=3$)	10 ± 1.0	13 ± 1.9	50% ($n=3$)	6 ± 1.2	12.7 ± 3.8	–	–	–
	Sp/C+	87.5% ($n=7$)	8 ± 1.1	12.9 ± 1.1	–	–	–	12.5% ($n=1$)	7	8
D60	Sp/C−	28.6% ($n=2$)	11	22 ± 1.5	14.3% ($n=1$)	9	21	57.1% ($n=4$)	6.0 ± 1.8	9.8 ± 1.4
	Sp/C+	62.5% ($n=5$)	11 ± 0.8	18.3 ± 0.6	12.5%($n=1$)	6	11	25% ($n=2$)	6.5 ± 0.5	9.5 ± 1.5

At D60, all repairs have been processed in three types (Table 1): *"total repair"* (Sp/C−: 28.6%; Sp/C+: 62.5%), *"partial repair"* (Sp/C−: 14.3%; Sp/C+: 12.5%) and *"hypertrophic repair"* (Sp/C−: 57.1%; Sp/C+: 25%). The percentage of *"total" repair"* was higher in the Sp/C+ group than in the Sp/C− group (62.5% versus 28.6%) thus leading for both groups to the improvement of macroscopic scores (Sp/C−:11; Sp/C+:11 ± 0.8). This repaired tissue presented a hyaline cartilage pattern with a smooth or occasionally rough aspect of its surface. Typically, low macroscopical scores characterized both "*partial repair*" (with a central hollow) and "*hypertrophic repair*" tissues, which showed a disorganized surface with hollows and bulging more frequently observed in the Sp/C− group (57.1%) versus the Sp/C+ group (25%).

Histology

At D20, *"total repairs"* presented an irregular surface with a junction at the same level of the adjacent cartilage while the rebuilding of the subchondral bone was not observed in the deep part. The repair tissue was characterized by a fibrotic pattern: an extracellular matrix weakly stained in PGs, strongly marked by picrosirius red (collagen) with a disorganized network in polarized-light microscopy. The phenotype of cells was fibroblastic like in the Sp/C− groups and chondrocyte like in the Sp/C+ group. *"Partial repairs"* were characterized by an irregular surface under the level of adjacent cartilage. Cell morphology and extracellular matrix characteristics were similar to those observed in the total repair groups.

At D40, for the Sp/C− groups, "*total and partial repairs"* presented a fibrotic pattern with a higher proportion of chondrocytes when compared with D20. A partial organization of the superficial part of the repair tissue was observed while, on the other hand, the deep zone was still disorganized. Conversely, in the Sp/C+ group, the number of chondrocytes was lower than D20 without modification of the extracellular matrix staining; additionally, the collagen network organization appeared in the deep part but was lacking in the superficial part. *"Hypertrophic repairs"* observed (Table 1) in the Sp/C+ group (12.5%), were characterized by a fibrotic pattern: fibroblastic cells, extracellular matrix weakly stained by toluidine blue (proteoglycan), but strongly marked by picrosirius red (collagen), with a disorganized collagen network under polarized light.

At D60, the *"total repairs"* in both groups were characterized by a chondrocyte phenotype associated with almost normal proteoglycan staining and only focal regions of matrix strongly marked by picrosirius red. In polarized light, the aspect of the superficial zone tended to be similar to a native cartilage. Concerning the medial and the deep zones, the collagen network presented some thick vertical fibers surrounding cells (Fig. 2). For both groups, we noted a progressive reconstruction of the subchondral bone near the margins of the defect. "*Hypertrophic repairs"* observed in the Sp/C− group (57.1%) and the Sp/C+ group (25%), were characterized by the same fibrotic pattern observed at D40 in Sp/C+.

T2 mapping of control

Qualitative

As shown previously, T2 mapping permitted the distinction of the cartilage, thin tissue in blue-green scale, recovering the subchondral bone, in black, from the trabecular bone in blue-green scale beneath the subchondral bone.

Quantitative

We noted a progressive and significant decrease of the T2 global values from 7.57 ± 0.35 ms to 6.48 ± 0.20 ms ($p < 0.05$) between D20 and D60 related to the maturation process of cartilage and ancillary biochemical variation of matrix content. A zonal variation of T2 values between the superficial (high T2 values) and the deep zones (lower T2 values) of the cartilage was also present at each time of the

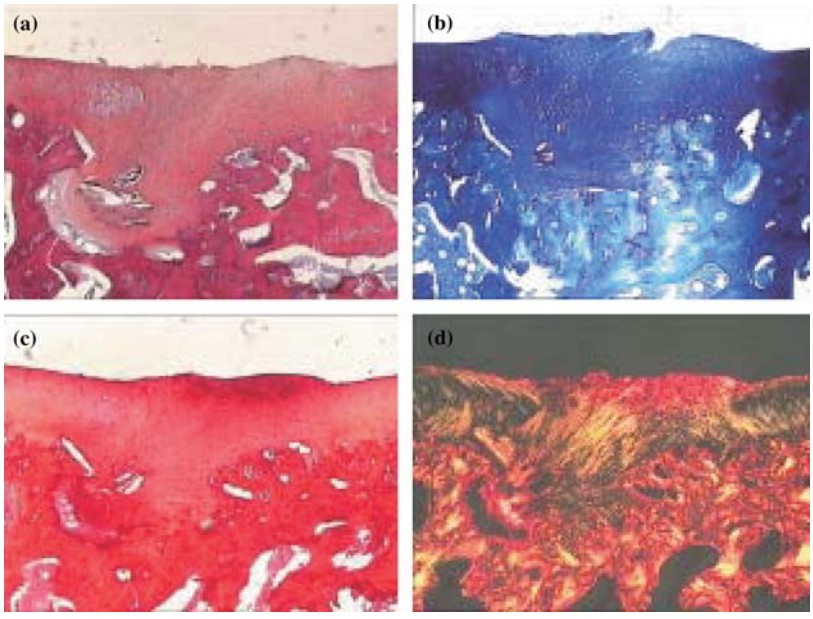

Fig. 2 Histological study (original magnification ×4) of healing areas at D60 in the "total repair" Sp/C+ group showing: **a** a cicatricial fibrocartilage recolonized by chondrocyte type cells **b** a quite normal proteoglycan staining **c** a focal region of matrix marked by picrosirius red (reflecting collagen content) **d** a collagen network organization almost normal in superficial and others zones with some thick vertical fibers (polarized light)

study (Fig. 3), inherent to the collagen network organization.

T2 mapping of repair groups

Morphological analysis

When the T2 mapping was realized at the level of the repair tissue, we noted a complete agreement between the macroscopic aspect and the superficial morphological aspect of the repaired zone observed in T2 mapping, whatever the stage considered. So, one also distinguished, as for the macroscopic analysis, three types of repairs. Total and partial repairs were observed at D20, D40 and D60 with a higher percentage of total repair tissue in Sp/C+ whatever the stage considered. The hypertrophic tissue appeared at D40 in the Sp/C+ group ($n = 1$) and was observed in both groups at D60 (predominantly in the Sp/C− group, 57.1% versus 25%). The repair tissue presented the same range of color (green to blue) in comparison to the adjacent normal cartilage, thus eliminating a delaminating process. T2 mapping also allowed one to obtain information about the internal structure of the repair tissue and to study the reconstruction of the bone-repair tissue interface, which could not be observed during a macroscopic analysis. In our experimental model, bone modifications, (lack of subchondral and trabecular bone disorganization) were present at D20 and D40. At D60, we noted a decrease of the trabecular bone disorganization and a reconstruction of the subchondral bone interface.

Quantitative analysis

"*Total repair" group*: At D20, The T2 global value in the Sp/C− group (7.57 ± 0.05 ms, $n = 2$) was similar to controls (7.57 ± 0.35 ms, $n = 8$). In the Sp/C+ group, the T2 global value was slightly higher 8.92 ± 0.78 ms, n=2). Additionally, no zonal variation of T2 values with cartilage depth was observed in both groups. At D40, the T2 global values of the Sp/C− group and much more the Sp/C+ group (7.82 ± 0.04 ms, $n = 3$; 10 ± 0.69 ms, $n = 7$, respectively) were statistically higher versus control (6.73 ± 0.16 ms, $n = 8$) ($p < 0.05$) without zonal variation in repair groups. Between D40 and D60, we noted a slight decrease of T2 global values in both repair groups, when compared with controls, which remained stable for this time period. Thus, at D60, T2 global values of Sp groups and especially the Sp/C+ group (7.31 ± 0.71 ms, $n = 2$; 9.08 ± 0.76 ms, $n = 5$) were still statistically higher versus control group (6.48 ± 0.20 ms, $n = 8$; $p < 0.05$). At this stage, a zonal variation of T2 values depending on cartilage depth ($p < 0.05$) was observed in repair groups but to a lesser extent versus control group.

"*Partial repair" group*: In the Sp/C− group, the T2 global values were statistically lower than controls and no zonal variation was observed at D20, D40 and D60. (Table 2). In the Sp/C+ group, partial repair was observed only at D20 ($n = 5$) and D60 ($n = 1$). In comparison to control groups, the T2 global values of the partial repair were slightly superior without statistical difference

Table 2 Global T2 values of repair tissues at D20, D40 and D60 following the type of repair tissue (total, partial and hypertrophic repair tissue) and the implanted scaffold (Sp/C– = Sponge Sp/C+ = Sponge with autologous chondrocytes). (*) $p < 0.05$ versus control

	Global T2 values (ms)						
	Normal cartilage	Total repair		Partial repair		Hypertrophic repair	
Time point	Control	Sp/C–	SP/C+	Sp/C–	SP/C+	Sp/C–	SP/C+
D20	7.57 ± 0.35 ($n = 8$)	7.57 ± 0.05 ($n = 2$)	8.92 ± 0.78 ($n = 2$)	2.76 ± 1.14 ($n = 3$) (*)	8.72 ± 1.13 ($n = 5$)	-	-
D40	6.73 ± 0.16 ($n = 8$)	7.82 ± 0.04 ($n = 3$) (*)	10.10 ± 0.69 ($n = 7$) (*)	4.82 ± 1.42 ($n = 3$) (*)	-	-	7.92 ($n = 1$)
D60	6.48 ± 0.20 ($n = 8$)	7.31 ± 0.71 ($n = 2$)	9.08 ± 0.76 ($n = 5$) (*)	5.34	7.86 ($n = 1$)	8.46 ± 0.23 ($n = 4$) (*)	8.90 ± 0.50 ($n = 2$) (*)

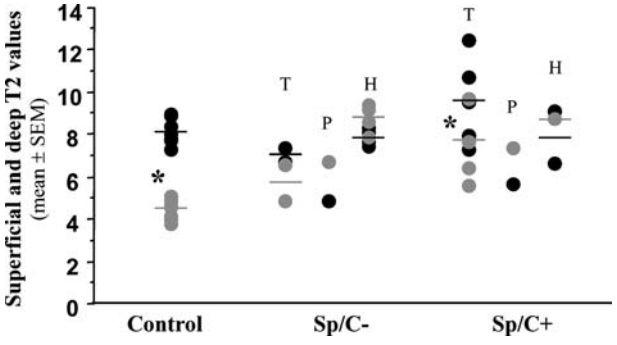

Fig. 3 Superficial (*black circle*) and deep (*gray circle*) T2 values (*zonal variation*) of repair tissues at D60. Significant difference (*$p < 0.05$) between superficial and deep zone were observed in control group ($n = 8$) and in the total (T) repair Sp/C+ group ($n = 5$). Please note that in hypertrophic (H) and partial (P) repair tissues no zonal variation was observed between the superficial and deep zones

(Table 2). Moreover, no zonal variation was observed between D20 and D60.

"*Hypertrophic repair" group* appeared at D40 for the Sp/C+ group and at D60 for both repair groups. The Sp/C– group and the Sp/C+ group ($n = 4$ and $n = 2$ respectively) were characterized by an increase of about 30% of their T2 global values when compared with controls (8.46 ± 0.23 ms and 8.90 ± 0.50 ms vs 6.48 ± 0.20 ms). As observed for partial repairs, no zonal variation was depicted in this type of tissue.

Discussion

We have developed a rat model of patellar cartilage defect, an anatomical structure for which T2 mapping, biochemical and histological data have previously been validated [7–9]. In the present study, we have explored the accuracy of T2 mapping at 8.5 T in characterizing cartilage repair tissue, a "tissue engineering" approach, after a chondral lesion in rat patella and the implantation of a biomaterial seeded or not with autologous chondrocytes. To date, macroscopic and histological studies remain the "gold standard" to characterize the type and the quality of the repair tissue at different time points, but are invasive in nature. The relevance of our model is based on the localization of this cartilage defect, patellar defects being the most frequent localization during knee OA [10], and on the fact that surgical coverage of this type of chondral defect, mosaicplasty [11] or chondrocytes graft [12] might be proposed at early stages before arthroplasty. Additionally, as an anatomical entity, patella can easily be explored ex vivo with high-field MRI at 8.5 T.

Numerous studies have been performed to study spontaneous repair in various experimental models of focal cartilage defects e.g. in rabbit [13], goat [14], dog [15] and rat [16, 17]. Recent works have also assessed the efficacy of different scaffolds containing embedded chondrocytes or multipotent stem cells to fill osteochondral defects [18–20]. In tissue engineering, several factors must be taken into account: (1) localization, depth and diameter of the chondral lesion, (2) the animal species considered, (3) the kind of scaffold and cells implanted, and (4) the programming of load impact after implantation. Additionally, concerning cartilage engineering, 3-D environment, as well as alginate-hyaluronate cell constructs, appear as a functional environment for embedded chondrocytes facilitating the production of an extracellular matrix (type II collagen) [21] and promoting chondrocyte phenotype preservation.

With this feature in mind, previous studies have explored the repair potential of the biopolymer alginate in focal cartilage lesion models in rabbits [22, 23] and rat [9]. Concerning the rat, in a cartilage defect performed on trochlear cartilage, as a non-load-bearing zone, Dausse et al. [9] demonstrated that such a scaffold implantation was well tolerated with no major effect on the spontaneous locomotor activity and body temperature of the animals. It is noteworthy that free motion after surgery did not affect the quality of the repair tissue and, even, could increase cartilage PG content as previously demonstrated by Espanha et al. [17] in a histological study performed

in the rat. Dausse et al. [9] have also demonstrated that "alginate sponge with hyaluronate" as well as "alginate sponges with hyaluronate and autologous chondrocytes" both led to a filling of the chondral defect. The histological score for total repair increase with time and the best score was obtained by the Sp/C+ group at D40, without hypertrophic tissue in the Sp/C− and Sp/C+ groups. Conversely, in the present work, hypertrophic tissue appeared at D40 in the Sp/C+ group but the percentage at D60 (25%) remained lower than the Sp/C− groups (57%). This fact is probably inherent to the defect localization and the kind of graft, corroborating Brittberg's findings related to human patellar grafts, where hypertrophic tissue was observed in 23% of autologous chondrocyte transplantation [12]. Histological studies of scared tissue by Dausse et al. [9] presented some hyaline-like area for Sp/C− and Sp/C+ with more proteoglycan staining and cell colonization and presence of organized collagen fiber for the latter. Our model corroborates this description except for the Sp/C− group for which collagen fiber organization appeared at D60 versus the Sp/C+ group which collagen fiber organization appeared at D40.

Currently, arthroscopy remains the validated technique to follow the cartilage repair tissue in clinical practice. But, this technique, invasive in nature, limits the number of longitudinal explorations. The development of non-invasive techniques therefore seems necessary for the future to evaluate longitudinally the different tissue engineering techniques dedicated to chondral lesions. Our previous study on spontaneous repair of a foal lesion of rat patellar cartilage [5] has confirmed the results of MR clinical studies [3, 24] using T2-weighted sequences, which permitted (1) the appreciation of the morphological evolution of grafts and (2) the differentiation of normal cartilage from delaminated or hypertrophic tissues.

Alparslan et al. [3] have followed the internal signal of chondrocyte graft, initially presenting an internal structure in hypersignal, before becoming normal one year later on T2-weighted sequences. Conversely, the hypertrophic and delaminated grafts remained in hypersignal throughout the study. Additionally, trabecular bone edema around the defect was in hypersignal at 12 months, but disappeared at 24 months. Thus, MRI appears to be able to assess the internal structure of repair tissue, to follow its evolution, and to evaluate cartilage-bone interface. Our study also confirmed the ability of T2 mapping to identify several morphological patterns previously described in the clinics: "*total*", "*partial*", and "*hypertrophic*" repair tissues [5].

When compared with clinical studies, delamination pattern was not observed on T2 mapping as well as on macroscopic and histological data. This particular point may be related to the fact that, in the present work, the defect is filled by a spongy scaffold which permits a blood clot issued from the subchondral bone, and not by a tissue graft as done in the clinics (mosaicplasty or autologous chondrocytes grafts). In all cases of repair tissue, a perilesional area characterized by high T2 values was observed in subchondral and trabecular bones.

As previously published [15], we noted in the control group a progressive and significant decrease of T2 global values between D20 and D60 and changes of cartilage matrix content inherent to the maturation process. "*Total repair*" tissue was characterized by high global T2 values versus age-matched control group. This higher T2 values is probably inherent to a chondral edema and a difference of matrix content versus control group. The histological analysis permits the confirmation of the macroscopic study and to observe qualitatively the matrix content, the cell phenotype and the collagen network organization. Additional biochemical studies of repair tissue are needed to determine quantitatively the extra-cellular matrix changes ancillary to the cicatrization process.

The zonal variation of T2 values (high T2 values in surface and low T2 values near the calcified cartilage) is classically observed in human cartilage as well as in numerous animal species [8, 10, 12, 24]. Recently, Nieminen et al. [26] have demonstrated that this zonal variation of T2 values was correlated ($r = 0.91$) with the collagen network organization on bovine osteochondral plugs. In our previous study, we have shown that this zonal variation of T2 values was also present in normal rat patellar cartilage as well as when repair tissue presented a collagen network organization. During pathologic repair, "hypertrophic tissue" and "partial repair", both pathologic and exerting no collagen network organization (partial), no zonal variation was depicted. Due to the high spatial resolution of this study, molecular diffusion during the sequence in presence of the imaging gradients could contribute to T2 decay and thus result in an under-evaluation of the T2 values found. After quantitative evaluation, this effect would at worst cause an under-evaluation by 5%, taking for the diffusion coefficient that of free water. Since this stays much smaller than the T2 variations obtained from our study, the apparent T2 map obtained should be representative of the pure T2 map.

Study limitations and clinical relevance

Several limitations of this pilot experimental study performed in the rat should be mentioned.

- The use of a quadruped model for the study of cartilage healing may introduce a bias in extrapolating data in bipeds. Nevertheless such rat models (young adult animals) have been validated previously by our group [5, 9] and others [27, 28]: they mimic over a short period (30–60 days) some histological and MR features of cartilage repair seen in the clinics (see [29] for review).

- Caution should be made to extrapolate these animal results to the clinics, because cartilage characterization is mainly confined to experimental or anatomical studies (published clinical MR assessments with concomitant second look and biopsies are scanty). Nevertheless, the major advantage of such experimental lesions is the possibility to monitor the course of the disease and to evaluate the potential interest of new biomaterials.
- Although this experimental study was performed at 8.5 T in the rat, our preliminary T2 maps of the patella performed at 1.5 T (GE Signa Echospeed) in healthy and OA patients demonstrate the accuracy of quantitative imaging in detecting post traumatic, age- and OA-related changes of patellar cartilage. In fact, in the near future, the extracellular matrix will be easily evaluated using T2 relaxation as a marker.

In conclusion, the results presented in this study confirm the potency of the MR T2 map (8.5 T) to characterize macroscopically and microscopically the patterns of the scaffold guided-tissue repair of a focal chondral lesion in the rat patella. Moreover, T2 map confirm its accuracy for characterizing with a good histological correlation several types of repair patterns ("total", "partial" and "hypertrophic") over 60 days, as we previously described extensively [5].

In the clinics, MRI is considered by most orthopaedists to be the optimal modality in assessing non-invasively articular cartilage after autologous chondrocyte implantation, being able to evaluate simultaneously the volume of repair tissue filling the cartilage defect, the restoration of the surface contour, the integration of the repair tissue to the subchondral plate, and the status of the subchondral bone [30]. In the same manner, MRI can reliably detect overgrowth or hypertrophy or graft delamination with a good histological delineation, as confirmed herein. Nevertheless, the use of MRI is limited by the lack of standardization and consensus on which sequences should be used. With this in mind, standardized "virtual biopsies" performed with T2 map, may help in assessing qualitatively and quantitatively cartilage healing.

We also demonstrated herein the chondrogenic potential of alginate sponges seeded with autologous chondrocytes (1) to produce an extracellular matrix with areas of hyaline aspect and (2) to prevent the appearance of hypertrophic tissue versus alginate and hyaluronate alone. With this in mind, MR T2 map may be performed on a focal region of interest, thus permitting (1) the acquisition of qualitative and quantitative parameters concerning the graft itself, depending on its kind and its location, and (2) the simultaneous analysis of adjacent tissues (cartilage and subchondral bone). MR macroscopic patterns, T2 global values and T2 zonal variation seem crucial to appreciate biochemical matrix content and evaluate the integrity of the collagen network organization, as well as its bio-integration and bio-functionality.

Finally, establishing objective, standardized outcome measures will be important to compare and assess future generations of treatment regimes incorporating scaffolds and support matrices, or other, more advanced, tissue-engineered therapies. With this in mind, T2 mapping is able to offer a "*MR biopsy*" able to evaluate, qualitatively and quantitatively, in vivo cartilage engineering maturation process whatever the type of graft. This parameter may be important for the post-operative control and evaluation of such treatment effects.

Acknowledgements The authors thank Venkatesan Narayanan for his expert advice, Stéphanie Etienne for her technical assistance and Michel Thiery for his good care to animals. This work was supported by grants from the Contrat de Projet de Recherche Clinique (2000), the « Fondation pour la Recherche Médicale », the "Région Lorraine", IT2B and ACI « CARTIGELIMAGE ».

References

1. Hunziker EB (2002) Articular cartilage repair: basic science and clinical progress. A review of the current status and prospects. Osteoarthritis Cartilage 10:432–463
2. Dougados M, Ayral X, Listrat V, et al. (1994) The SFA system for assessing articular cartilage lesions at arthroscopy of the knee. Arthroscopy 10:69–77
3. Alparslan L, Minas T, Winalski CS (2001) Magnetic resonance imaging of autologous chondrocyte implantation. Semin Ultrasound CT MR 22:341–351
4. Azer NM, Winalski CS, Minas T (2004) MR imaging for surgical planning and postoperative assessment in early osteoarthritis. Radiol Clin North Am 42:43–60
5. Watrin-Pinzano A, Ruaud JP, Cheli Y, et al (2004) T2 mapping: an efficient MR quantitative technique to evaluate spontaneous cartilage repair in rat patella. Osteoarthritis Cartilage 12:191–200
6. Mlynarik V, Szomolanyi P, Toffanin R, Vittur F, Trattnig S (2004) Transverse relaxation mechanisms in articular cartilage. J Magn Reson.169:300–307
7. Watrin A, Ruaud JP, Olivier PT, et al. (2001) T2 mapping of rat patellar cartilage. Radiology 219:395–402
8. Loeuille D, Olivier P, Watrin A, et al. (2002) The biochemical content of articular cartilage: an original MRI approach. Biorheology 39:269–276

9. Dausse Y, Grossin L, Miralles G, et al. (2003) Cartilage repair using new polysaccharidic biomaterials: macroscopic, histological and biochemical approaches in a rat model of cartilage defect. Osteoarthritis Cartilage 11:16–28
10. McAlindon TE, Snow S, Cooper C, Dieppe PA (1992) Radiographic patterns of osteoarthritis of the knee joint in the community: the importance of the patellofemoral joint. Ann Rheum Dis 51:844–849
11. Hangody L, Rathonyi GK, Duska Z, Vasarhelyi G, Fules P, Modis L (2004) Autologous osteochondral mosaicplasty. Surgical technique. J Bone Joint Surg Am 86A:65–72
12. Brittberg M, Lindahl A, Nilsson A, Ohlsson C, Isaksson O, Peterson L (1994) Treatment of deep cartilage defects in the knee with autologous chondrocyte transplantation. N Engl J Med 331:889–895
13. Mooney V, Ferguson AB Jr (1966) The influence of immobilization and motion on the formation of fibrocartilage in the repair granuloma after joint resection in the rabbit. J Bone Joint Surg Am 48:1145–1155
14. Jackson DW, Lalor PA, Aberman HM, Simon TM (2001) Spontaneous repair of full-thickness defects of articular cartilage in a goat model. A preliminary study. J Bone Joint Surg Am 83A:53–64
15. Breinan HA, Martin SD, Hsu HP, Spector M (2000) Healing of canine articular cartilage defects treated with microfracture, a type-II collagen matrix, or cultured autologous chondrocytes. J Orthop Res 18:781–789
16. Yoshioka M, Kubo T, Coutts RD, Hirasawa Y (1998) Differences in the repair process of longitudinal and transverse injuries of cartilage in the rat knee. Osteoarthritis Cartilage 6:66–75
17. Espanha MM, Lammi PE, Hyttinen MM, Lammi MJ, Helminen HJ (2001) Extracellular matrix composition of full-thickness defect repair tissue is little influenced by exercise in rat articular cartilage. Connect Tissue Res 42:97–109
18. Ibusuki S, Iwamoto Y, Matsuda T (2003) System-engineered cartilage using poly(N-isopropylacrylamide)-grafted gelatine as in situ-formable scaffold: in vivo performance. Tissue Eng 9:1133–1142
19. Wakitani S, Goto T, Young RG, Mansour JM, Goldberg VM, Caplan AI (1998) Repair of large full-thickness articular cartilage defects with allograft articular chondrocytes embedded in a collagen gel. Tissue Eng 4:429–444
20. Im GI, Kim DY, Shin JH, Hyun CW, Cho WH (2001) Repair of cartilage defect in the rabbit with cultured mesenchymal stem cells from bone marrow. J Bone Joint Surg Br 83:289–294
21. Miralles G, Baudoin R, Dumas D, et al. (2001) Sodium alginate sponges with or without sodium hyaluronate: in vitro engineering of cartilage. J Biomed Mater Res 57:268–278
22. Mierisch CM, Wilson HA, Turner MA, et al. (2003) Chondrocyte transplantation into articular cartilage defects with use of calcium alginate: the fate of the cells. J Bone Joint Surg Am 85A(9):1757–1767
23. Fragonas E, Valente M, Pozzi-Mucelli M, et al. (2000) Articular cartilage repair in rabbits by using suspensions of allogenic chondrocytes in alginate. Biomaterials 21:795–801
24. Sanders TG, Mentzer KD, Miller MD, Morrison WB, Campbell SE, Penrod BJ (2001) Autogenous osteochondral "plug" transfer for the treatment of focal chondral defects: postoperative MR appearance with clinical correlation. Skeletal Radiol 30:570–578
25. Goodwin DW (2001) Visualization of the macroscopic structure of hyaline cartilage with MR imaging. Semin Musculoskelet Radiol 5:305–312
26. Nieminen MT, Rieppo J, Toyras J, et al. (2001) T2 relaxation reveals spatial collagen architecture in articular cartilage: a comparative quantitative MRI and polarized light microscopic study. Magn Reson Med 46:487–493
27. Nishida T, Kubota S, Kojima S, et al. (2004) Regeneration of defects in articular cartilage in rat knee joints by CCN2 (connective tissue growth factor). J Bone Miner Res 19:1308–1319
28. Kawasaki K, Sugihara S, Nishida K, et al. (2004) Hoechst 33342 is a useful cell tracer for a long-term investigation of articular cartilage repair. Arch Histol Cytol. 67:13–19
29. Verstraete KL, Almqvist F, Verdonk P, et al. (2004) Magnetic resonance imaging of cartilage and cartilage repair. Clin Radiol 59:674–689
30. Roberts S, McCall IW, Darby AJ, Menage J, Evans H, Harrison PE, Richardson JB (2003). Autologous chondrocyte implantation for cartilage repair: monitoring its success by magnetic resonance imaging and histology. Arthritis Res Ther 5:R60–R73